

## MIT Open Access Articles

*Effect of annealing on magnetic properties in ferrimagnetic GdCo alloy films with bulk perpendicular magnetic anisotropy*

The MIT Faculty has made this article openly available. **Please share** how this access benefits you. Your story matters.

**Citation:** Ueda, Kohei et al., "Effect of annealing on magnetic properties in ferrimagnetic GdCo alloy films with bulk perpendicular magnetic anisotropy." AIP Advances 8, 12 (December 2018): 125204 ©2018 Authors

**As Published:** <https://dx.doi.org/10.1063/1.5054164>

**Publisher:** AIP Publishing

**Persistent URL:** <https://hdl.handle.net/1721.1/128665>

**Version:** Final published version: final published article, as it appeared in a journal, conference proceedings, or other formally published context


**Terms of use:** Creative Commons Attribution 4.0 International license



# Effect of annealing on magnetic properties in ferrimagnetic GdCo alloy films with bulk perpendicular magnetic anisotropy <sup>EP</sup>

Cite as: AIP Advances **8**, 125204 (2018); <https://doi.org/10.1063/1.5054164>

Submitted: 30 August 2018 . Accepted: 25 November 2018 . Published Online: 04 December 2018

Kohei Ueda , Aik Jun Tan, and Geoffrey S. D. Beach

## COLLECTIONS

 This paper was selected as an Editor's Pick



View Online



Export Citation



CrossMark

## ARTICLES YOU MAY BE INTERESTED IN

[Spin-orbit torque-induced switching in ferrimagnetic alloys: Experiments and modeling](#)  
Applied Physics Letters **112**, 062401 (2018); <https://doi.org/10.1063/1.5017738>

[Spin-orbit torques in ferrimagnetic GdFeCo alloys](#)  
Applied Physics Letters **109**, 112403 (2016); <https://doi.org/10.1063/1.4962812>

[Spin-orbit torques in Ta/Tb<sub>x</sub>Co<sub>100-x</sub> ferrimagnetic alloy films with bulk perpendicular magnetic anisotropy](#)  
Applied Physics Letters **109**, 232403 (2016); <https://doi.org/10.1063/1.4971393>



**Flexible RF Cabling  
for Cryogenic Setups**

[www.delft-circuits.com](http://www.delft-circuits.com)

## Effect of annealing on magnetic properties in ferrimagnetic GdCo alloy films with bulk perpendicular magnetic anisotropy

Kohei Ueda,<sup>a,b</sup> Aik Jun Tan, and Geoffrey S. D. Beach<sup>c</sup>

*Department of Materials Science and Engineering, Massachusetts Institute of Technology, Cambridge, Massachusetts 02139, USA*

(Received 30 August 2018; accepted 25 November 2018; published online 4 December 2018)

Magnetic properties in ferrimagnetic GdCo alloy films with bulk perpendicular magnetic anisotropy (PMA) are investigated as a function of annealing temperature ( $T_{\text{anneal}}$ ) and annealing time for several capping layers. Magnetic properties in films capped by TaO<sub>x</sub> vary markedly with  $T_{\text{anneal}}$ ; the saturation magnetization and coercivity vary progressively with increasing  $T_{\text{anneal}}$  up to 300 °C, and above that temperature, PMA is lost abruptly. By comparing the annealing temperature dependence for Co-dominated and Gd-dominated compositions close to the magnetization compensation point, the data are readily explained by preferential oxidation of Gd during annealing. When films are capped by a Ta/Pt bilayer, the film properties are stable up  $T_{\text{anneal}} = 300$  °C, indicating that oxidation at high temperatures is effectively blocked, but the abrupt loss of PMA for  $T_{\text{anneal}} > 300$  °C is still observed. X-ray diffraction measurement reveals that the amorphous structure of the films remains the same after high-temperature annealing that is sufficient to remove PMA, indicating that crystallization from the amorphous phase is not responsible for the lack of PMA. Instead, our results suggest that high annealing temperatures may cause segregation of Co and Gd atoms in the films, which reduces anisotropic pair-pair correlations responsible for the observed bulk PMA in the as-grown state. © 2018 Author(s). All article content, except where otherwise noted, is licensed under a Creative Commons Attribution (CC BY) license (<http://creativecommons.org/licenses/by/4.0/>). <https://doi.org/10.1063/1.5054164>

Current-induced spin-orbit torques (SOTs) in ferromagnets in contact with heavy metal layers with strong spin-orbit coupling<sup>1–13</sup> have gained considerable attention due to their potential for memory and logic devices.<sup>14</sup> Recent work has focused on transition metal (TM)-rare earth metal (RE) ferrimagnetic alloys. These ferrimagnets are antiferromagnetically exchange coupled systems with antiparallel TM and RE sub-lattices. It has been shown that ferrimagnet/heavy-metal bilayers exhibit effective SOTs<sup>15–25</sup> that trigger magnetization switching<sup>17,19,22,24,25</sup> and magnetic domain wall motion<sup>16,23</sup> when in contact with a heavy metal. The net magnetization of the ferrimagnet can be tuned by controlling its composition and temperature, and there exists a magnetic compensation point where the ferrimagnet exhibits zero net magnetization. At this point, the magnetization of the two sub-lattices are equal in the magnitude but opposite in direction. Although the coercivity diverges at magnetic compensation, precluding switching by magnetic fields, current-induced SOTs remain finite since the corresponding effective fields scale inversely with the magnetization.<sup>17,20–22,25</sup> Hence, SOT-based devices can be operated in materials with compensated sublattices where the net magnetization vanishes and stray fields can be eliminated, which is desirable for applications.

RE-TM ferrimagnets came to prominence four decades ago<sup>26–45</sup> as magneto-optical recording media, where they have usually been studied in the form of rather thick films in which interfaces

<sup>a</sup>Present address: Department of Physics, Osaka University, Machikaneyama, Toyonaka, Osaka 560-0043, Japan

<sup>b</sup>[kueda@phys.sci.osaka-u.ac.jp](mailto:kueda@phys.sci.osaka-u.ac.jp)

<sup>c</sup>[gbeach@mit.edu](mailto:gbeach@mit.edu)

are less important. By contrast, in ferrimagnet/heavy-metal structures that exploit spin-orbit coupling effects, thin and ultrathin films are more suitable, in which case effects at interfaces such as intermixing, alloy segregation, and interface oxidation, become much more important. A particularly useful property in these amorphous-like ferrimagnets is the presence of perpendicular magnetic anisotropy (PMA) with a bulk-like behavior. There have been many suggestions as to the possible mechanisms which lead to PMA in these materials, including magnetostriction,<sup>33</sup> anisotropic pair correlation,<sup>27,28,38,39</sup> dipolar effects,<sup>30,36</sup> and bond-orientation anisotropy.<sup>35</sup> Furthermore, it has been found that the magnetic properties of RE-TM thin films are highly sensitive to growth conditions (Ar flow rate during deposition,<sup>43</sup> substrate choice,<sup>40</sup> external strain,<sup>41</sup> etc.) as well as annealing procedure.<sup>29</sup> The ferrimagnetic layer thickness is also a critical factor which may change the magnetic compensation due to the formation of boundary layers at the interface of cap and bottom layers.<sup>31,32,45</sup> Despite many reports on the properties, there are still many unanswered questions. For example, growing ferrimagnetic alloys on partially oxidized substrates changes the thickness threshold for attaining PMA, as well as other magnetic properties.<sup>18,44</sup> Moreover, adjacent oxide layers can influence the magnetic properties during annealing.<sup>29</sup> These issues motivate careful examination of the effects of annealing and capping layers on the properties of thin-film RE-TM alloys, especially for thin film structures in which the behavior at interfaces is particularly important. Further understanding of ferrimagnetic properties is indispensable in order to realize spin orbitronics applications based on TM-RE ferrimagnetic films.

In this report we present systematic characterization of magnetic properties in thin ferrimagnetic GdCo alloy films by investigating the effect of annealing temperature and annealing time. To isolate the effects of oxidation, we studied films capped by an oxide layer (TaO<sub>x</sub>) and a noble metal (Ta/Pt). We find that magnetic properties in films with a TaO<sub>x</sub> cap layer show a progressive change with increasing annealing temperature,  $T_{\text{anneal}}$ , below 300 °C, consistent with preferential oxidation of Gd, and a much more pronounced change above 350 °C that includes an abrupt loss of PMA. By contrast, for films with a Ta/Pt cap layer, the magnetic properties are stable up to 300°C, suggesting oxidation is greatly reduced, but the abrupt loss of PMA above this threshold still occurs. X-ray diffraction (XRD) measurements show that the amorphous structure remains the same before and after annealing, indicating that structural transformation to a crystalline phase is not responsible for the loss of PMA. We suggest that instead, high-temperature annealing disrupts anisotropic pair-pair correlations, which have been previously been found to contribute as a source of structural anisotropy in RE-TM films.<sup>27,28,38,39</sup> These results provide evidence for the microscopic origin of PMA in these films and identify processing limitations that may be important for their implementation into complementary metal oxide semiconductor-compatible spintronic devices.

We prepared multilayers comprising Ta(3)/Pt(4)/Gd<sub>x</sub>Co<sub>100-x</sub>(8)/cap on top of SiO<sub>2</sub>/Si substrates by room temperature dc magnetron sputtering (Fig. 1(a)). Here, the numbers in parentheses are

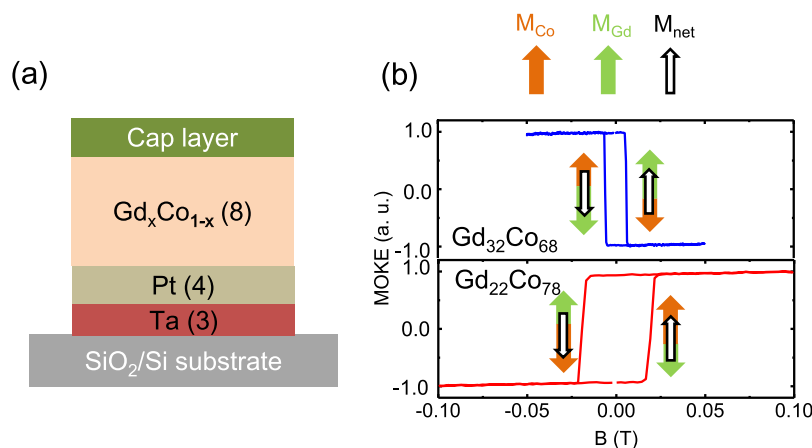


FIG. 1. (a) Schematic illustration of layer structure (b) Magneto-optical Kerr effect loops for Co-dominated (Gd<sub>22</sub>Co<sub>78</sub>) and Gd-dominated (Gd<sub>32</sub>Co<sub>68</sub>) films in the as-deposited state.

thicknesses in nm, and  $x$  indicates the atomic percent of Gd in the GdCo alloy. The capping layers were either TaO<sub>x</sub>(3) or Ta(4)/Pt(3). In the former case, the TaO<sub>x</sub> cap is prepared by natural oxidation of a 3nm thick Ta overlayer, whereas in the latter case, the top Pt layer inhibits oxidation. The bottom Ta layer serves as an adhesion layer. Gd<sub>x</sub>Co<sub>100-x</sub> alloys were grown by co-sputtering at 3 mTorr Ar pressure with a background pressure of  $\sim 1 \times 10^{-7}$  Torr. We examined films with  $x=22$  and  $x=32$ , yielding compositions that are slightly RE-rich and slightly RE-poor, compared to the composition yielding magnetization compensation at room temperature. Figure 1(b) shows out-of-plane hysteresis loops measured by the magneto-optical Kerr effect, which demonstrate the perpendicular anisotropy of TaO<sub>x</sub>-capped films of each composition at room temperature. The inversion of the Kerr signal for the two samples confirms that they are on either side of compensation, since the Kerr signal tracks the transition metal sublattice,<sup>46</sup> which orients parallel (antiparallel) to the net magnetization below (above) compensation.

We first examine the effects of annealing on the magnetic properties of Co-dominated and Gd-dominated films capped by TaO<sub>x</sub>. For each specimen, experiments were performed by annealing the sample under flowing argon in ambient air at a temperature  $T_{\text{anneal}}$  for 30 minutes and then returning the sample to room temperature for magnetic property characterization. Data were obtained by sequentially increasing the annealing temperature between measurements on the same specimen, with annealing temperatures ranging from 100 °C to 400 °C in 50 °C increments. To obtain the magnetic properties, magnetization curves in the out-of-plane (OOP) and in-plane (IP) directions were measured using a vibrating sample magnetometer (VSM). We measured the coercive field ( $\mu_0 H_C$ ) of the easy axis magnetization curve, the saturation magnetization ( $M_S$ ), and the hard-axis saturation field ( $B_K^{\text{eff}}$ ). We computed the effective magnetic anisotropy energy density ( $K_U^{\text{eff}}$ ) and the uniaxial magnetic anisotropy energy density ( $K_U$ ) through the following relations:

$$K_U^{\text{eff}} = \frac{(B_K^{\text{eff}} M_S)}{2}, \quad (1)$$

$$K_U = K_U^{\text{eff}} + \mu_0 M_S^2 / 2. \quad (2)$$

Figure 2 shows OOP and IP magnetization curves measured for the Co-dominated film capped by TaO<sub>x</sub> in the as-deposited state and after annealing at various  $T_{\text{anneal}}$ . These films exhibit PMA in the virgin state and after  $T_{\text{anneal}}$  up to 300 °C (Fig. 2(a),(c)), and exhibit in-plane magnetic anisotropy (IMA) for  $T_{\text{anneal}} = 350$  °C and 400 °C (Fig. 2(b),(d)). We see that  $M_S$  increases with  $T_{\text{anneal}}$  from  $8 \times 10^4$  A/m in its virgin state up to  $\sim 1.7 \times 10^5$  A/m at  $T_{\text{anneal}} = 300$  °C. At  $T_{\text{anneal}} = 350$  °C and 400 °C where the film exhibits IMA, the  $M_S$  increases further to  $\sim 4.8 \times 10^5$  A/m. Figure 3 shows corresponding results for Gd-dominated film capped by TaO<sub>x</sub>. Similar to the case of the Co-dominated film in Fig. 2, PMA is retained for  $T_{\text{anneal}}$  up to 300 °C and lost at higher  $T_{\text{anneal}}$ . However, in contrast to the Co-dominated case,  $M_S$  exhibits a nonmonotonic behavior with respect to  $T_{\text{anneal}}$ .

Figure 4 summarizes  $\mu_0 H_C$ ,  $M_S$ ,  $K_U^{\text{eff}}$  and  $K_U$  as a function of  $T_{\text{anneal}}$  for the Co and Gd-dominated films capped by TaO<sub>x</sub>. First, we focus on the regime with  $T_{\text{anneal}}$  up to 300 °C where PMA is retained. As shown in Figs. 4(a),(b), as  $T_{\text{anneal}}$  increases, for the Co-dominated film,  $\mu_0 H_C$  decreases monotonically while  $M_S$  increases. By contrast, for the Gd-dominated film,  $\mu_0 H_C$  first increases and then decreases, whereas  $M_S$  exhibits the opposite trend. We find a dramatic increase of  $\mu_0 H_C$  at  $T_{\text{anneal}}=250$  °C, where  $M_S$  takes a minimum. This behavior is reminiscent of the hysteresis behavior as a RE-TM film is brought through compensation either by temperature or composition. Since in this case the magnetic properties are always measured isothermally, the results indicate that the annealing process is changing the composition, similar to what has been suggested in previous annealing studies.<sup>29</sup>

Indeed, our results are explained quite naturally by preferential oxidation of the RE element, Gd, at higher  $T_{\text{anneal}}$ . At low temperature, the TaO<sub>x</sub> cap acts as a passivation layer that protects the film from further oxidation, but at elevated temperatures, the oxide growth kinetics change<sup>47</sup> and the oxide layer thicknesses increases by partial oxidation of the GdCo film below. Since the rare earth element is expected to oxidize more readily compared to Co due to its smaller electronegativity,<sup>44</sup> the Gd metal would preferentially oxidize, decreasing the Gd content  $x$  in the Gd<sub>x</sub>Co<sub>100-x</sub> alloy. In the case of an initially Co-dominated composition, decreasing  $x$  decreases the net moment of the

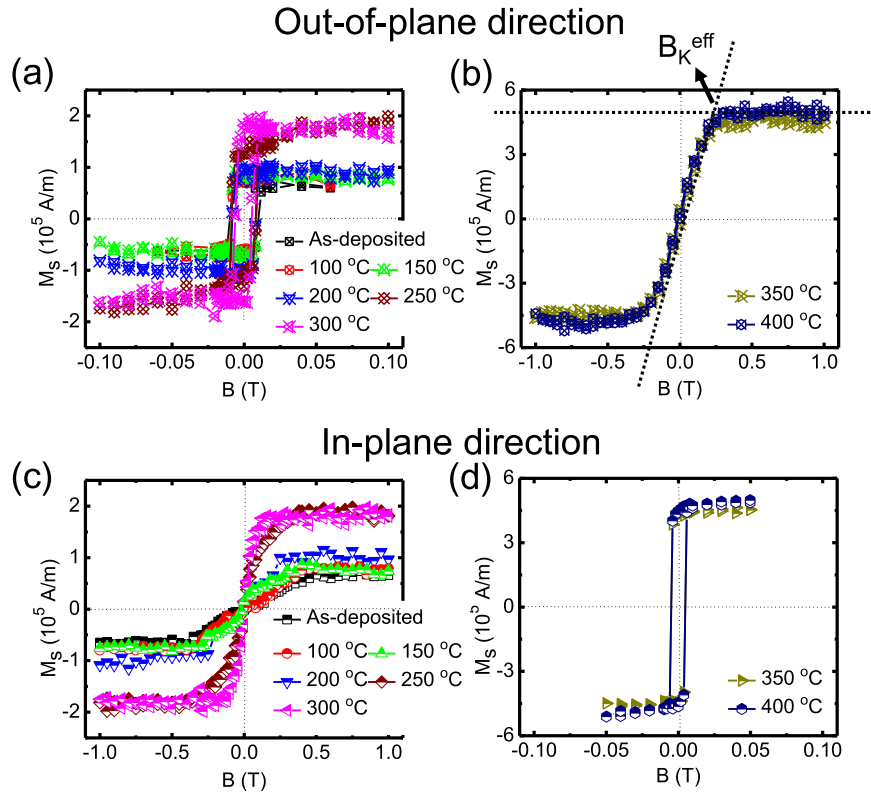


FIG. 2. Out-of-plane magnetization curves for Co-dominated film capped by  $\text{TaO}_x$  in (a) as-deposited state and after annealing at  $T_{\text{anneal}}=100\text{--}300$  °C, and after (b)  $T_{\text{anneal}}=350$  °C and 400 °C. In-plane magnetization curves for Co-dominated film in (c) as-deposited state and after  $T_{\text{anneal}}=100\text{--}300$  °C and (d)  $T_{\text{anneal}}=350$  °C and 400 °C.

RE sublattice that is antiparallel to the net magnetization, so  $M_s$  should increase monotonically, just as we observe. In the case of an initially RE-dominated film, progressive oxidation of Gd would bring the composition closer and closer to compensation, leading to reduction of  $M_s$  and divergence of  $\mu_0 H_C$ , until the composition becomes Co rich, at which point the trends in  $\mu_0 H_C$  and  $M_s$  would reverse. This also is exactly what we observe.

We now turn to the abrupt loss of PMA for  $T_{\text{anneal}} > 300$  °C, manifesting as the sign change of  $K_U^{\text{eff}}$  from positive to negative in Fig. 4(c). One might anticipate that since there is a considerable increase in  $M_s$  coincident with the transition from out-of-plane to in-plane magnetization (Fig. 4(b)), that the increased demagnetizing fields counteract the uniaxial anisotropy and drive the magnetization in-plane. However, as is seen in Fig. 4(d), when the demagnetization energy is accounted for,  $K_U$  still shows the same behavior, indicating that a loss of bulk PMA unrelated to annealing-induced oxidation or composition variation is responsible.

To verify this, we performed similar annealing studies using a sample with a Ta(3)/Pt(3) cap to minimize the effects of oxidation. Here, we measured the magnetic properties as a function of annealing time at two temperatures, 250 °C and 400 °C, which are above, and below the PMA-IMA transition temperature observed in Fig. 5(a)–(d). In addition, the lower annealing temperature was sufficient to cause significant oxidation-induced changes in the  $\text{TaO}_x$ -capped sample, as seen in Fig. 4. In Fig. 5(a)–(d), we show the magnetic properties ( $\mu_0 H_C$ ,  $M_s$ ,  $K_U^{\text{eff}}$  and  $K_U$ ) as a function of annealing time, where it is seen that the properties are stable at 250 °C for at least 120 minutes of annealing, whereas at 400 °C, the PMA is lost. The stability at lower annealing temperature confirms that the Ta/Pt cap effectively prevents oxidation, and the oxidation-induced property changes observed in the case of the  $\text{TaO}_x$  cap. Nonetheless, the high-temperature loss of PMA as well as the significant enhancement in  $M_s$  is still observed.

These results suggest that the loss of PMA and increase in  $M_s$  induced by annealing above 300 °C has a structural origin. Possible temperature-induced structural changes include crystallization of the

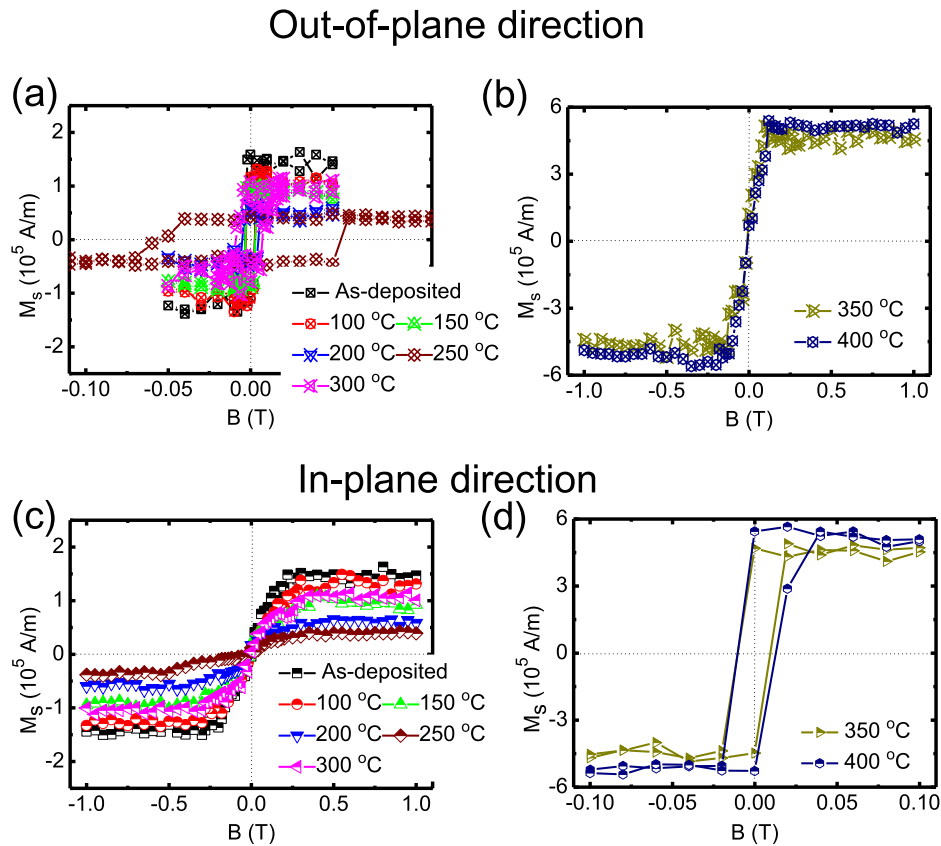


FIG. 3. Out-of-plane magnetization curves for Gd-dominated film capped by TaO<sub>x</sub> in (a) as-deposited state and after annealing at  $T_{\text{anneal}}=100\text{--}300\text{ }^{\circ}\text{C}$ , and after (b)  $T_{\text{anneal}}=350\text{ }^{\circ}\text{C}$  and  $400\text{ }^{\circ}\text{C}$ . In-plane magnetization curves for Gd-dominated film in (c) as-deposited state and after  $T_{\text{anneal}}=100\text{--}300\text{ }^{\circ}\text{C}$  and (d)  $T_{\text{anneal}}=350\text{ }^{\circ}\text{C}$  and  $400\text{ }^{\circ}\text{C}$ .

amorphous phase, and disruption of local anisotropy pair ordering, both of which could potentially disrupt PMA. In the as-deposited case, RE-TM alloys are known to be amorphous, which is usually associated with the observation of PMA in such films, and high-temperature annealing could result in crystallization to an ordered phase. Alternatively, anisotropic pair-pair correlations, which are believed to play an important role in bulk PMA in amorphous RE-TM alloys,<sup>27,28,38,39</sup> could also be disrupted by chemical segregation at higher temperature. To explore these possibilities, we performed grazing-incidence x-ray diffraction (XRD) measurements on a Si/SiO<sub>2</sub>/Ta(4)/Pt(3)/GdCo(8)/Ta(3)/Pt(3) film in the as-deposited state and after annealing at  $400\text{ }^{\circ}\text{C}$  for 30 min. Figure (5e) shows a standard  $2\theta$  diffraction pattern measured at fixed grazing incidence. Crystalline Pt peaks can be seen, whereas no other peaks besides those attributable to the substrate are observed either before or after annealing. The lack of any identifiable GdCo peaks provides evidence for its amorphous nature both before and after annealing, despite the crossover between PMA and IMA, which was independently observed in this sample using VSM measurements. We also performed XRD measurements on a thicker (100nm) GdCo layer and again found no evidence of crystallinity before or after annealing (Fig. 5(f)).

This observation suggests that any induced structural changes are subtle and not easily detected using XRD. Harris *et al.* have shown clear evidence of structural anisotropy in ferrimagnetic TbFe exhibiting bulk PMA, indicating the preference for Tb-Fe pair correlation in the OOP direction, and for Fe-Fe and Tb-Tb pair correlations in the IP directions, and this anisotropic pair correlation decreases with high annealing temperature.<sup>38</sup> Further studies by same group confirmed that PMA enhancement with the structural anisotropy is associated with increased Tb-Fe pair correlation.<sup>39</sup> Similarly, atomic pair ordering has also been shown to play a crucial role in generating bulk PMA in GdCo alloys.<sup>27,28</sup> Following the above scenario and our experimental studies, we conclude that the loss of PMA in the films studied here is most likely due to atomic reordering where segregation

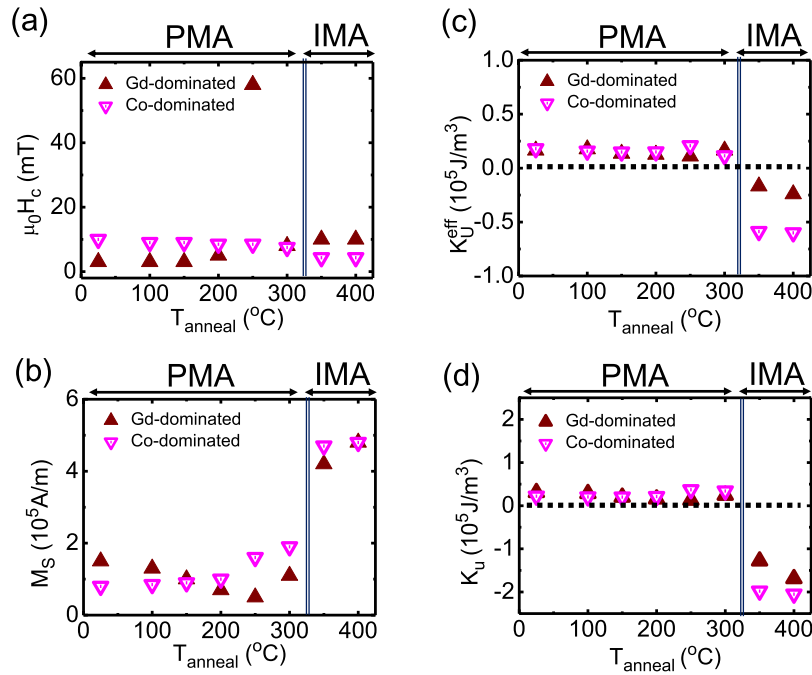


FIG. 4. (a) Coercive field ( $\mu_0 H_c$ ), (b) saturation magnetization ( $M_s$ ), (c) effective magnetic anisotropy energy density ( $K_U^{\text{eff}}$ ), (d) magnetic anisotropy energy density ( $K_U$ ) as a function of annealing temperature for Co-dominated and Gd-dominated films.

of Gd and Co atoms causes the weakening of Gd-Co pair correlations in the OOP direction. Such segregation could also explain the sharp increase in  $M_s$  for annealing temperatures above  $300^\circ\text{C}$ , in that the formation of Co-rich regions with higher  $M_s$  could enhance the volume averaged  $M_s$  of the composite film.

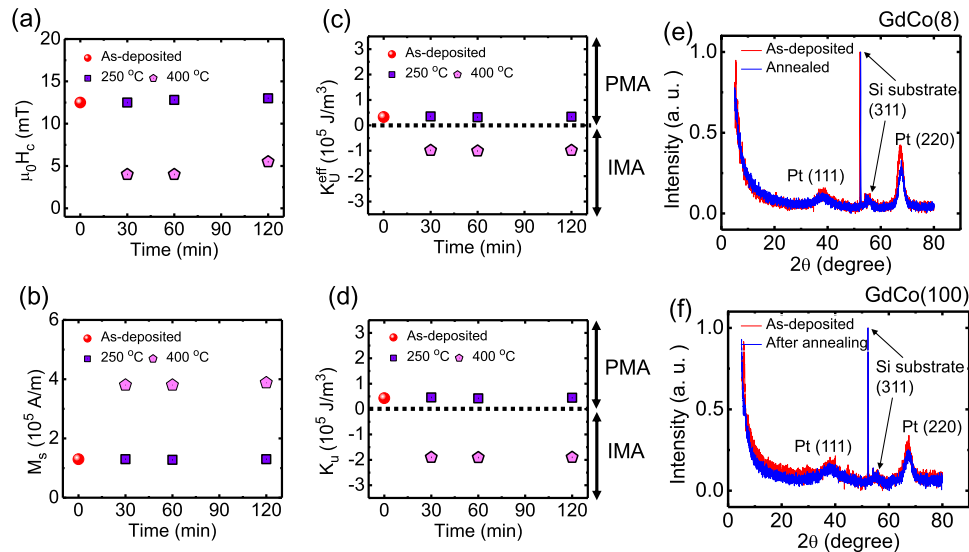


FIG. 5. Effects of annealing on Ta/Pt capped sample. (a) Coercive field ( $\mu_0 H_c$ ), (b) saturation magnetization ( $M_s$ ), (c) effective magnetic anisotropy energy density ( $K_U^{\text{eff}}$ ), (d) magnetic anisotropy energy density ( $K_U$ ) as a function of annealing time for  $250^\circ\text{C}$  and  $400^\circ\text{C}$ . Red circles indicate as-deposited films. X-ray diffraction scans of Si/SiO<sub>2</sub>/Ta(4)/Pt(4)/GdCo( $t_{\text{GdCo}}$ )/Ta(3)/Pt(3) films in the as-deposited state and after annealing at  $400^\circ\text{C}$  for 30 minutes for (e)  $t_{\text{GdCo}}=8$  nm, and (f)  $t_{\text{GdCo}}=100$  nm.



In summary, we have examined the magnetic properties of ferrimagnetic GdCo alloy films with bulk PMA as a function of annealing temperature and annealing time using different cap layers (TaO<sub>x</sub> and Ta/Pt). For GdCo/TaO<sub>x</sub> films, the data suggest progressive oxidation of Gd during annealing, leading to a changing alloy composition and correspondingly-changing properties. When annealed above 300°C, however, the changes are much more abrupt, with PMA vanishing and the saturation magnetization increasing significantly. When the TaO<sub>x</sub> cap is replaced by Ta/Pt, the film is effectively protected by oxidation at elevated temperature, but the abrupt loss of PMA for annealing above 300°C is still observed. X-ray diffraction measurements provide no indication of crystallization of the amorphous GdCo at these high annealing temperatures, which suggests that anisotropic pair-pair correlations may be dominantly responsible for the bulk PMA and that this atomic pair ordering is unstable at moderate annealing temperatures. More studies are required to directly examine pair ordering in this system, but, these results provide important insights into the stability of magnetic properties in thin-film RE-TM films at elevated temperature. The experimental insights will be important for designing RE-TM ferrimagnetic thin-film heterostructures for spin-orbitronics applications.

We would like to thank Dr. Charles Settens for his assistance with XRD measurement and fruitful discussion. This work made use of the MRSEC Shared Experimental Facilities at MIT, supported by the National Science Foundation under award number DMR-14-19807. This work was also supported by the National Science Foundation under NSF-ECCS-1408172.

- <sup>1</sup> M. Miron, K. Garello, G. Gaudin, P.-J. Zermatten, M. V. Costache, S. Auffret, S. Bandiera, B. Rodmacq, A. Schuhl, and P. Gambardella, *Nature* **476**, 189 (2011).
- <sup>2</sup> L. Liu, C.-F. Pai, Y. Li, H. W. Tseng, D. C. Ralph, and R. A. Buhrman, *Science* **336**, 555 (2012).
- <sup>3</sup> C.-F. Pai, L. Liu, Y. Li, H. W. Tseng, D. C. Ralph, and R. A. Buhrman, *Appl. Phys. Lett.* **101**, 122404 (2012).
- <sup>4</sup> K. Garello, I. M. Miron, C. O. Avci, F. Freimuth, Y. Mokrousov, S. Blügel, S. Auffret, O. Boulle, G. Gaudin, and P. Gambardella, *Nat. Nanotechnol.* **8**, 587 (2013).
- <sup>5</sup> J. Kim, J. Sinha, M. Hayashi, M. Yamanouchi, S. Fukami, T. Suzuki, S. Mitani, and H. Ohno, *Nat. Mater.* **12**, 240 (2013).
- <sup>6</sup> C. O. Avci, K. Garello, C. Nistor, S. Godey, B. Ballesteros, A. Mugarza, A. Barla, M. Valvidares, E. Pellegrin, A. Ghosh, I. M. Miron, O. Boulle, S. Auffret, G. Gaudin, and P. Gambardella, *Phys. Rev. B* **89**, 214419 (2014).
- <sup>7</sup> S. Woo, M. Mann, A.-J. Tan, L. Caretta, and G. S. D. Beach, *Appl. Phys. Lett.* **105**, 212404 (2014).
- <sup>8</sup> Q. Hao and G. Xiao, *Phys. Rev. B* **91**, 224413 (2015).
- <sup>9</sup> T. Nan, S. Emori, C.-T. Boone, X. Wang, T.-M. Oxholm, J.-G. Jones, B.-M. Howe, G.-J. Brown, and N.-X. Sun, *Phys. Rev. B* **91**, 214416 (2015).
- <sup>10</sup> M.-H. Nguyen, D. C. Ralph, and R. A. Buhrman, *Phys. Rev. Lett.* **116**, 126601 (2016).
- <sup>11</sup> C.-F. Pai, M. Mann, A. J. Tan, and G. S. D. Beach, *Phys. Rev. B* **93**, 144409 (2016).
- <sup>12</sup> K. Ueda, C.-F. Pai, A. J. Tan, M. Mann, and G. S. D. Beach, *Appl. Phys. Lett.* **108**, 232405 (2016).
- <sup>13</sup> A. Ghosh, K. Garello, C. O. Avci, M. Gabureac, and P. Gambardella, *Phys. Rev. Appl.* **7**, 014004 (2017).
- <sup>14</sup> S.-H. Yang, K.-S. Ryu, and S. Parkin, *Nat. Nanotechnol.* **10**, 221 (2015).
- <sup>15</sup> Z. Zhao, M. Jamali, A. K. Smith, and J.-P. Wang, *Appl. Phys. Lett.* **106**, 132404 (2015).
- <sup>16</sup> D. Bang, J. Yu, X. Qiu, Y. Wang, H. Awano, A. Manchon, and H. Yang, *Phys. Rev. B* **93**, 174424 (2016).
- <sup>17</sup> J. Finley and L. Liu, *Phys. Rev. Applied* **6**, 054001 (2016).
- <sup>18</sup> K. Ueda, M. Mann, C.-F. Pai, A.-J. Tan, and G. S. D. Beach, *Appl. Phys. Lett.* **109**, 232403 (2016).
- <sup>19</sup> R. Mishra, J. Yu, X. Qiu, M. Motapothula, T. Venkatesan, and H. Yang, *Phys. Rev. Lett.* **118**, 167201 (2017).
- <sup>20</sup> K. Ueda, M. Mann, P. W. P. de Brouwer, D. Bono, and G. S. D. Beach, *Phys. Rev. B* **96**, 064410 (2017).
- <sup>21</sup> W. S. Ham, S. Kim, D.-H. Kim, K.-J. Kim, T. Okuno, H. Yoshikawa, A. Tsukamoto, T. Moriyama, and T. Ono, *Appl. Phys. Lett.* **110**, 242405 (2017).
- <sup>22</sup> N. Roschewsky, C.-H. Lambert, and S. Salahuddin, *Phys. Rev. B* **96**, 064406 (2017).
- <sup>23</sup> Y. Kurokawa, A. Shibata, and H. Awano, *AIP Advances* **7**, 055917 (2017).
- <sup>24</sup> T.-C. Wang, T.-Y. Chen, C.-T. Wu, H.-W. Yen, and C.-F. Pai, *Phys. Rev. Mater.* **2**, 014403 (2018).
- <sup>25</sup> S.-G. Je, J.-C. Rojas-Sanchez, T. H. Pham, P. Vallobra, G. Malinowski, D. Lacour, T. Fache, M.-C. Cyrille, D.-Y. Kim, S.-B. Choe, M. Belmeguenai, M. Hehn, S. Mangin, G. Gaudin, and O. Boulle, *Appl. Phys. Lett.* **112**, 062401 (2018).
- <sup>26</sup> P. Chaudhari, J. J. Cuomo, and R. J. Gambino, *Appl. Phys. Lett.* **22**, 337 (1973).
- <sup>27</sup> R. C. Taylor and A. Gangulee, *J. of Appl. Phys.* **47**, 4666 (1976).
- <sup>28</sup> R. J. Gambino and J. J. Cuomo, *J. Vac. Sci. Technol.* **15**, 296 (1978).
- <sup>29</sup> T. Katayama, K. Hasegawa, K. Kawamishi, and T. Tsushima, *J. Appl. Phys.* **49**, 1759 (1978).
- <sup>30</sup> T. Mizoguchi and G. S. Cargill III, *J. Appl. Phys.* **50**, 3570 (1979).
- <sup>31</sup> R. Malmhäll and T. Chen, *J. Appl. Phys.* **53**, 7843 (1982).
- <sup>32</sup> M. Nakada, K. Toki, and M. Okada, *IEEE Trans. Magn.* **2**, 348 (1987).
- <sup>33</sup> S.-C. N. Cheng, M. H. Kryder, and M. C. A. Mathur, *IEEE Trans. Magn.* **25**, 4018 (1989).
- <sup>34</sup> P. Hansen, G. Clausen, G. Much, M. Rosenfranz, and K. Witter, *J. Appl. Phys.* **66**, 756 (1989).
- <sup>35</sup> X. Yan, M. Hirscher, T. Egami, and E. E. Marinero, *Phys. Rev. B* **43**, 9300 (1991).
- <sup>36</sup> H. Fu, M. Mansuripur, and P. Meystre, *Phys. Rev. Lett.* **66**, 1086 (1991).
- <sup>37</sup> F. Hellman and E. M. Gyorgy, *Phys. Rev. Lett.* **68**, 1391 (1992).
- <sup>38</sup> V. G. Harris, K. D. Aylesworth, B. N. Das, W. T. Elam, and N. C. Koon, *Phys. Rev. Lett.* **69**, 13 (1992).

- <sup>39</sup> V. G. Harris, W. T. Elam, and N. C. Koon, *Phys. Rev. B* **49**, 5 (1994).
- <sup>40</sup> S. M. Na, S. J. Suh, and S. H. Lim, *J. Appl. Phys.* **93**, 8507 (2003).
- <sup>41</sup> M. Ohta, K. Yamada, Y. Satake, A. Fujita, and K. Fukamichi, *Mater. Trans.* **44**, 2605 (2003).
- <sup>42</sup> M. T. Rahman, X. Liu, and A. Morisako, *J. Magn. Magn. Mater.* **303**, 133 (2006).
- <sup>43</sup> H. C. Jiang, W. L. Zhang, W. X. Zhang, and B. Peng, *Physica B Condens. Matter* **405**, 834 (2010).
- <sup>44</sup> S. Q. Yin, X. Q. Li, X. G. Xu, J. Miao, and Y. Jiang, *IEEE Trans. Mag.* **47**, 10 (2011).
- <sup>45</sup> B. Hebler, A. Hassdenteufel, P. Reinhard, H. Karl, and M. Albrecht, *Front. Mater.* **3**, 8 (2016).
- <sup>46</sup> P. Hansen and H. Heitmann, *IEEE Trans. Magn.* **25**, 4390 (1989).
- <sup>47</sup> A. T. Fromhold and E. L. Cook, *Phys. Rev.* **158**, 600 (1967).